Available online at www.sciencedirect.com
ScienceDirect
Thin Solid Films 516 (2008) 2869–2873
thin solid films
www.elsevier.com/locate/tsf

Deep etch-induced damage during ion-assisted chemical etching of sputtered indium–zinc–oxide films in $Ar/CH_4/H_2$ plasmas

L. Stafford [a,*], W.T. Lim [a], S.J. Pearton [a], Ju-Il Song [b], Jae-Soung Park [b], Young-Woo Heo [b], Joon-Hyung Lee [b], Jeong-Joo Kim [b], M. Chicoine [c], F. Schiettekatte [c]

[a] Department of Materials Science and Engineering, University of Florida, Gainesville, FL, 32611, USA
[b] Department of Inorganic Materials Engineering, Kyungpook National University, Daegu, 702-701, Republic of Korea
[c] Département de Physique, Université de Montréal, Montréal, Québec, Canada H3C 3J7

Received 14 January 2007; received in revised form 19 May 2007; accepted 24 May 2007
Available online 9 June 2007

Abstract

Plasma etch damage to sputtered indium–zinc–oxide (IZO) layers in the form of changes in the film stoichiometry was investigated using Auger Electron Spectroscopy (AES). While damage resulting from pure chemical etching processes is usually constrained to the surface vicinity, ion-assisted chemical etching of IZO in $Ar/CH_4/H_2$ plasmas produces a Zn-rich layer, whose thickness (~50 nm) is well-above the expected stopping range of Ar ions in IZO (~1.5 nm). Based on AES depth profiles as a function of plasma exposure time, it is concluded that the observed Zn enrichment and In depletion deep into the IZO film are driven by the implantation of hydrogen atoms.

Keywords: Plasma etching; Damage; Transparent conducting oxides; Implantation; Auger Electron Spectroscopy; Indium–zinc–oxide

1. Introduction

The development of reliable pattern transfer processes is one of the critical issues for the integration of functional thin films relevant for applications in electronics, optoelectronics, and photonics. Among the various patterning techniques, plasma etching is preferred because it allows high resolution pattern transfer for device structures. One drawback of this method is the formation of damage upon plasma exposure that often degrades device performance. Depending on the material etched and the plasma chemistry used, the damage may take the form of point defects and their complexes, changes in near-surface stoichiometry, presence of residual etch products or deposition of polymers. A number of experiments have confirmed the presence of these various forms of etch-induced damage using electrical, optical, and structural characterization techniques [1–12]. For physical sputtering, depth profile measurements have indicated that the damage induced by low ion energy bombardment can extend deeper than the predicted ion stopping range because of both ion channeling and defect diffusion [9–13]. On the other hand, for pure chemical etching processes the damage is usually restrained to the surface vicinity due to the expected low diffusion coefficients under typical room-temperature etching conditions.

In this work, we examine the mechanisms of plasma-induced damage to sputtered indium–zinc–oxide (IZO) films during ion-assisted chemical etching in reactive plasma chemistries. Because of their good electrical conductivity, wide transmittance window, large work function, excellent surface smoothness, and low deposition temperature, IZO films have recently emerged as a very promising material for transparent electrodes in optoelectronic devices such as liquid crystal displays, light-emitting diodes, and solar cells [14–17]. In contrast to pure chemical etching processes, it is shown that changes in the IZO film stoichiometry upon preferential desorption of group III etch products can extend much deeper than the surface vicinity. Possible mechanisms for the formation of such deep etch-induced damage are discussed.

* Corresponding author.
E-mail address: sluc@mse.ufl.edu (L. Stafford).

0040-6090/$ - see front matter © 2007 Elsevier B.V. All rights reserved.
doi:10.1016/j.tsf.2007.05.071

2. Experimental details

IZO films were deposited on glass substrates (Corning EAGLE2000) using radio frequency magnetron sputtering. The $In_2O_3(ZnO)_2$ target was fabricated using high purity In_2O_3 (99.99%) and ZnO(99.9%) by a conventional ceramic processing technique [18]. Sputter-deposition was carried out at room temperature with an argon pressure of 10 mTorr and a sputtering power of 50 W. The distance between target and substrate was fixed to 70 mm. The sample composition was analyzed by Rutherford Backscattering Spectroscopy (RBS) using a 4.57 MeV $^4He^{++}$ ion beam. The angle between the He beam and the surface normal was 7° to minimize channeling. The detector was placed at a scattering angle of 170°. We found an indium-to-zinc atomic composition ratio of ~1.3. The concentration fraction of oxygen atoms was 56±2%, which is similar to that expected from the $In_2O_3(ZnO)_2$ target.

High-density plasma etching of IZO films was realized using an Oerlikon (formerly Unaxis) 790 Inductively Coupled Plasma (ICP) reactor. The 2 MHz power applied to the ICP source and the 13.56 MHz chuck power were held constant at 300 W and 200 W, respectively. Etching was performed in $Ar/CH_4/H_2$ plasma chemistries, the mass flow rates (in standard cubic centimeters per minutes (sccm)) being $3CH_4$, $10H_2$ and 8Ar. The total gas pressure before plasma ignition was set to 0.67 Pa. Under these conditions, the energy of the ions impinging onto the material was ~320 eV. This ion energy was calculated by the sum of self-bias voltage and sheath potential (about 25 V for the ICP source under investigation).

Auger Electron Spectroscopy (AES) was used to analyze the plasma-induced damage. A Physical Electronics 660 Auger Microprobe Electron Beam at 10 keV, 0.3 μA, 30° from sample normal was used for the data collection while for depth profiling the ion beam conditions were 3 keV Ar^+, 2.0 μA, and $(4\ mm)^2$ raster with sputter-etch rate of 86 Å/min (SiO_2). A survey spectrum (a plot of the first derivative of the number of electrons detected as a function of energy) was used to determine the composition of the outer few nanometers of each sample. Quantifications were accomplished by using elemental sensitivity factors. Prior to data acquisition, secondary electron images (SEIs) were obtained to document analysis area and surface morphology.

3. Experimental results and discussion

Fig. 1 presents the AES depth profiles as a function of plasma exposure time, t, for Zn (top) and In (bottom) atoms. While as-grown IZO samples have homogeneous depth profiles with concentration fractions similar to those determined by RBS, it can be seen that after etching in $Ar/CH_4/H_2$, the concentration of Zn progressively increases in the near-surface region, becoming larger than that of In for $t \geq 60$ s. Fig. 1 further shows that the thickness of the altered surface region slightly increases between $t=30$ s and $t=60$ s, and then *drastically* increases afterwards, reaching ~50 nm at $t=120$ s. This is well-above the expected stopping range of Ar ions in $In_{1.3}Zn_1O_3$ (~1.5 nm) determined from standard ion range simulators such as Stopping-and-Range-of-Ions-in-Matter (SRIM) [19].

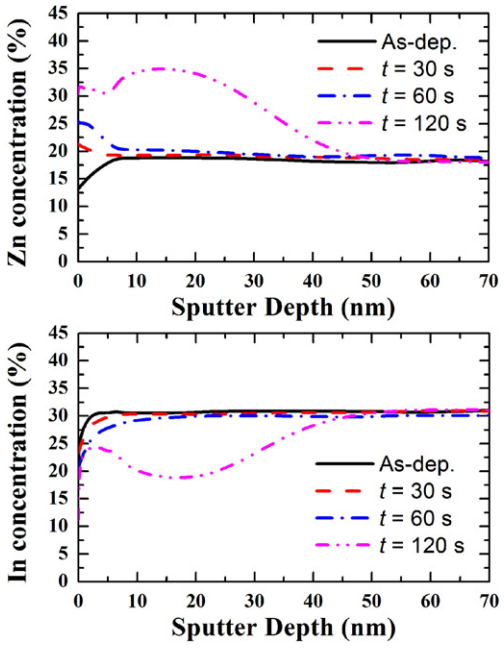

Fig. 1. AES depth profiles of Zn (top) and In (bottom) of IZO films after etching in $Ar/CH_4/H_2$ plasma.

SEIs from as-deposited and post-etched IZO surfaces are shown in Fig. 2a–d. While SEIs from as-deposited (Fig. 2a) and 30 s-etched (Fig. 2b) IZO samples show relatively smooth surfaces, Fig. 2c and d indicate considerable surface roughening due to the formation of particle-like features. The presence of such features on post-etched surfaces has also been observed for the etching of other multi-component materials such as InP and $(Ba,Sr)TiO_3$ in $CH_4/H_2/Ar$ and Ar/Cl_2 plasma chemistries, respectively (see for example [20–22]). These features can be attributed to the preferential desorption of one reaction products, for example $TiCl_4$ for $(Ba,Sr)TiO_3$ etching in Ar/Cl_2 plasmas [21]. Based on the AES depth profiles presented in Fig. 1, the surface roughening observed in Fig. 2 for $t \geq 60$ s can thus be understood in terms of preferential desorption of In-containing reaction products.

For most plasma etching experiments reported in the literature, changes in the film stoichiometry upon preferential desorption of one reaction product are restrained to the very near-surface region. There are several mechanisms that may explain the unusual deep etch-induced damage displayed in Fig. 1. The first one involves the acceleration or deceleration of the etch rate with plasma exposure time. However, Fig. 3 clearly shows that the IZO etch depth exhibits a fairly linear variation with t, indicating that this mechanism cannot explain the presence of etch-induced damage beyond the surface vicinity. Another mechanism routinely invoked for deep sputtering-induced damage is channeling of the ions along a low-index direction of the crystal [9–13]. However, our separate X-ray diffraction analysis has shown that the room-temperature-deposited IZO layers under investigation are essentially amorphous [23,24], which indicates that ion channeling is unlikely to occur.

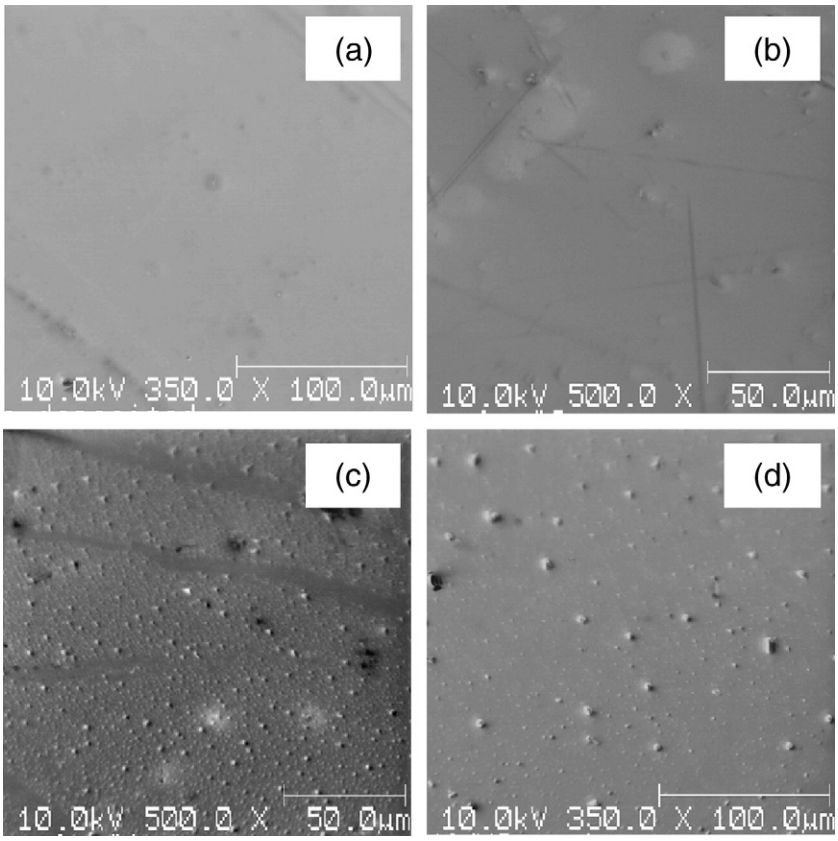

Fig. 2. SEIs from as-deposited and post-etched IZO films (a) as-deposited, (b) $t=30$ s, (c) $t=60$ s, and (d) $t=120$ s.

The deep etch-induced damage observed in Fig. 1 could also result from diffusion. Based on Fick's diffusion law, one would indeed expect In atoms to diffuse from the bulk to the surface to smooth the gradients resulting from the preferential desorption of the group-III etch products. Similarly, there is accumulation of Zn in the near-surface region due to the slow desorption of Zn-containing reaction products so that Zn atoms should counter-diffuse. Note that for $t=120$ s, Fig. 1 shows a minimum in the In profile whereas a maximum is observed for Zn, these features being *a priori* difficult to understand from diffusion arguments alone. This behavior can probably be attributed to polymer deposition at the topmost surface during etching in CH_4-containing plasmas which retards the desorption of reaction products, and therefore inhibits the diffusion process [25,26]. In this framework, using the results presented in Fig. 1 for $t=120$ s and assuming a typical Gaussian profile in the 20–70 nm range where polymer deposition can be neglected, one can roughly estimate a diffusion coefficient in the 10^{-14}–10^{-13} $cm^2\ s^{-1}$ range. This is clearly much higher than the expected thermal diffusion coefficients of any metal in any oxide (see for example [27]). Moreover, the thickness of the altered surface region presented in Fig. 1 drastically increases between 60 s and 120 s, which is inconsistent with the time dependence expected from a simple Fickian diffusion process.

The presence of such threshold-like behavior in the evolution of etch-induced damage between $t=60$ s and $t=120$ s suggests that an additional time-dependent phenomenon is driving the diffusion dynamics. Among possible phenomenon, the drastic change in the Zn and In concentration fractions deep into the IZO layer for high t can probably be attributed to the

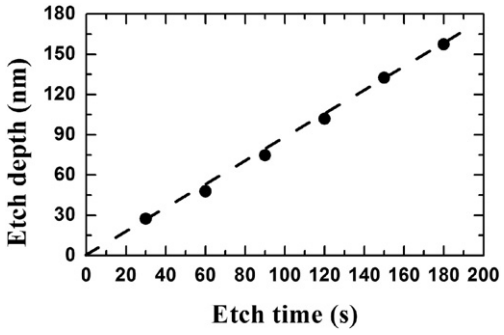

Fig. 3. Influence of the plasma exposure time on the etch depth of IZO.

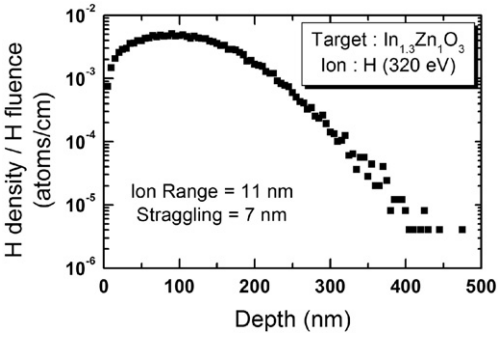

Fig. 4. Simulated depth profile of implanted hydrogen atoms.

introduction of hydrogen in the film upon exposure to the Ar/CH_4/H_2 plasma. Indeed, based on SRIM 2003 simulations [19], Fig. 4 shows that hydrogen ions with energy ~320 eV impinging onto $In_{1.3}Zn_1O_3$ films can penetrate as deep as 40 nm with range and straggling of 11 and 7 nm, respectively. In addition, it was shown by Ip et al. [28] that hydrogen atoms are likely to diffuse in plasma hydrogenated ZnO even for relatively low temperatures (25–250 °C). For example, incorporation depths of >10 μm were obtained in 0.5 h at 100 °C. Deep penetration of H atoms was also demonstrated in other materials for similar plasma etching conditions (see for example Refs. [29–32]). This very high diffusivity of hydrogen atoms at such low temperatures results from the fact that H transport in larger host atom matrixes is driven by a direct interstitial mechanism for which the activation energy is relatively low [33,34]. Based on these results, it is therefore expected that upon exposure to the Ar/CH_4/H_2 plasma, hydrogen atoms are implanted deeply into the IZO layer.

In the high-density Ar/CH_4/H_2 plasma under investigation, one may roughly estimate an hydrogen ion flux in the 10^{15} cm^{-2} s^{-1} range, yielding a hydrogen fluence of ~10^{17} cm^{-2} for t=120 s. This fluence is clearly high enough to form extended hydrogen-related damage such as embrittlement, blistering, or even cracking of the IZO layer [35–37]. Indeed, recent micro-Raman spectroscopy measurements by R. Job [38] have shown that plasma hydrogenation of ZnO produced nanovoids due to the formation of H_2 molecules. Cathodoluminescence measurements performed on the same samples also showed significant intensity variations which can be correlated to structural damage and morphological changes of the ZnO. Considering the deep penetration of H atoms evidenced above, these results suggest that extended hydrogen-related damage is also present deep into the IZO layers.

At this point, it is not clear which transport mechanism driven by hydrogen-related damage is more likely responsible for the deep Zn accumulation and In depletion during ion-assisted chemical etching of rf-sputtered IZO layers in Ar/CH_4/H_2 plasmas. A possible candidate is enhanced In diffusion/Zn counter-diffusion due to the expected fast transport along nanovoids or blisters boundaries [39]. However, other mechanisms could also be involved. Still, given the depth range where the changes in the film stoichiometry appear and the non-linearity of the phenomenon with plasma exposure time (i.e. hydrogen fluence), this transport mechanism must be related to the damage generated by the implantation of hydrogen atoms.

4. Conclusion

In summary, we have shown that for the etching of sputtered IZO layers in Ar/CH_4/H_2 plasmas, changes in the near-surface stoichiometry upon preferential desorption of the group-III etch products can extend much deeper than the near surface region. Given the depth range where the etch-induced damage appears and the non-linearity of the phenomenon with plasma exposure time, this mechanism was found to be related to the implantation of hydrogen atoms. Note that these results are expected to be applicable to the etching of other multi-component materials in other hydrogenated plasma chemistries, provided the system under investigation allows sufficient preferential desorption of one of the elements.

Acknowledgments

This research was sponsored by the Army Research Office (ARO) under Grant No. DAAD19-01-1-0603, the National Science Foundation (NSF) under Grants Nos. DMR 0400416, 0305228 (L. Hess), the Department of Energy (DOE) under Grant No. DE-FC26-04NT42271, the DOE contract No. DE-AC05-00OR22725, and by the Air Force Office of Scientific Research (AFOSR) under Grant No. F49620-03-1-0370. This work was also supported by the National Research Laboratory grant from the Ministry of Science and Technology (MOST) and Korea Science and Engineering Foundation (KOSEF). The work at UdeM was funded by the Natural Science and Engineering Research Council (NSERC) and by the Fonds Québécois de la Recherche sur la Nature et les Technologies (FQRNT). One of the authors (L.S.) would like to acknowledge the financial support from the NSERC post-doctoral fellowship program.

References

[1] M. Rahman, L.G. Deng, C.D.W. Wilkinson, J.A. van den Berg, J. Appl. Phys. 89 (2001) 2096.
[2] X.A. Cao, A.P. Zhang, G.T. Dang, F. Ren, S.J. Pearton, R.J. Shul, L. Zhang, J. Vac. Sci. Technol., A, Vac. Surf. Films 18 (2000) 1144.
[3] P.K. Gadgil, T.D. Mantei, X.C. Mu, J. Vac. Sci. Technol., B 12 (1994) 102.
[4] H.S. Yang, S.Y. Han, K.H. Baik, S.J. Pearton, F. Ren, Appl. Phys. Lett. 86 (2005) 102104.
[5] H.W. Choi, C. Liu, M.G. Cheong, J. Zhang, S.J. Chua, Appl. Phys., A 80 (2005) 405.
[6] G. Morello, M. Quaglio, G. Meneghini, C. Papuzza, C. Kompocholis, J. Vac. Sci. Technol., B 24 (2006) 756.
[7] R. Cheung, S. Withanage, R.J. Reeves, S.A. Brown, I. Ben-Yaacov, C. Kirchner, M. Kamp, Appl. Phys. Lett. 74 (1999) 3185.
[8] N.G. Stoffel, S.A. Schwarz, M.A.A. Pudensi, K. Kash, L.T. Florez, J.P. Harbison, B.J. Wilkens, Appl. Phys. Lett. 60 (1992) 1603.
[9] E.L. Hu, C.-H. Chen, D.L. Green, J. Vac. Sci. Technol., B 14 (1996) 3632.
[10] F. Frost, K. Otte, A. Schindler, F. Bigl, G. Lippold, V. Gottschalch, Appl. Phys. Lett. 71 (1997) 1362.
[11] E.D. Haberer, C.-H. Chen, A. Abare, M. Hansen, S. Denbaars, L. Coldren, U. Mishra, E.L. Hu, Appl. Phys. Lett. 76 (2000) 3941.
[12] E.D. Haberer, C.H. Chen, M. Hansen, S. Keller, S.P. Den Baars, U.K. Mishra, E.L. Hu, J. Vac. Sci. Technol., B 19 (2001) 603.
[13] M. Rahman, J. Appl. Phys. 82 (1997) 2215.
[14] G. Hu, B. Kumar, H. Gong, E.F. Chor, P. Wu, Appl. Phys. Lett. 88 (2006) 101901.
[15] A. Shah, P. Torres, R. Tscharner, N. Wyrsch, H. Keppner, Science 285 (1999) 692.
[16] H.K. Kim, K.S. Lee, J.H. Kwon, Appl. Phys. Lett. 88 (2006) 012103.
[17] K. Ramamoorthy, K. Kumar, R. Chandramohan, K. Sankaranarayanan, Mater. Sci. Eng., B, Solid-State Mater. Adv. Technol. 126 (2006) 1.
[18] K.Y. Son, D.H. Park, J.H. Lee, J.J. Kim, J.S. Lee, Solid State Ionics 172 (2004) 425.
[19] J.F. Ziegler, J.P. Biersack, U. Littmark, The Stopping and Range of Ions in Solids, Pergamon, New York, 1985.
[20] H.M. Lee, D.C. Kim, W. Jo, K.Y. Kim, J. Vac. Sci. Technol., B 16 (1998) 1891.
[21] T. Shibano, T. Takenaga, K. Nakamura, T. Oomori, J. Vac. Sci. Technol., A, Vac. Surf. Films 18 (2000) 2080.
[22] J.A. Diniz, J.W. Swart, K.B. Jung, J. Hong, S.J. Pearton, Solid State Electron 42 (1998) 1947.

[23] J.S. Park, J.I. Song, Y.W. Heo, J.H. Lee, W.T. Lim, L. Stafford, D.P. Norton, S.J. Pearton, J.J. Kim, J. Vac. Sci. Technol., B 24 (2006) 2737.
[24] L. Stafford, W.T. Lim, S.J. Pearton, M. Chicoine, S. Gujrathi, F. Schiettekatte, J.I. Song, J.S. Park, Y.W. Heo, J.H. Lee, J.J. Kim, J. Vac. Sci. Technol., A, Vac. Surf. Films 25 (2007) 659.
[25] G.S. Oehrlein, Surf. Sci. 386 (1997) 222.
[26] M. Schaepkens, T.E.F.M. Standaert, N.R. Rueger, P.G.M. Sebel, G.S. Oehrlein, J.M. Cook, J. Vac. Sci. Technol., A, Vac. Surf. Films 17 (1999) 26.
[27] C.Y. Wong, F.S. Lai, Appl. Phys. Lett. 48 (1986) 1658.
[28] K. Ip, M.E. Overberga, K.W. Baik, R.G. Wilson, S.O. Kucheyev, J.S. Williams, C. Jagadish, F. Ren, Y.W. Heo, D.P. Norton, J.M. Zavada, S.J. Pearton, Solid State Electron 47 (2003) 2255.
[29] G.S. Oehrlein, R.M. Tromp, J.C. Tsang, Y.H. Lee, E.J. Petrillo, J. Electrochem. Soc. 132 (1985) 1441.
[30] R.G. Wilson, S.J. Pearton, C.R. Abernathy, J.M. Zavada, J. Vac. Sci. Technol., A, Vac. Surf. Films 13 (1985) 719.
[31] M. Ezaki, Y. Kato, T. Tojo, J. Vac. Sci. Technol., B 19 (2001) 2911.
[32] S.J. Pearton, J.C. Zolper, R.J. Shul, F. Ren, J. Appl. Phys. 86 (1999) 1.
[33] R. Kirchheim, Prog. Mater. Sci. 32 (1988) 261.
[34] K. Ip, M.E. Overberg, Y.W. Heo, D.P. Norton, S.J. Pearton, C.E. Stutz, S.O. Kucheyev, C. Jagadish, J.S. Williams, B. Luo, F. Ren, D.C. Look, J.M. Zavada, Solid State Electron 47 (2003) 2289.
[35] W.K. Chu, R.H. Kastl, R.F. Lever, S. Mader, B.J. Masters, Phys. Rev., B 16 (1977) 3851.
[36] J.-K. Lee, Y. Lin, Q.X. Jia, T. Höchbauer, H.S. Jung, L. Shao, A. Misra, M. Nastasi, Appl. Phys. Lett. 89 (2006) 101901.
[37] R. Singh, R. Scholz, U. Gösele, S. Christiansen, Proc. Mater. Res. Soc. 957 (2006) K09-01.
[38] R. Job, Proc. Mater. Res. Soc. 957 (2006) K10-40.
[39] R.W. Baluffi, S.M. Allen, W.C. Carter, Kinetics of Materials, Wiley, New Jersey, 2005.